

Oleg Malkov* and Alexey Kniazev

Wide binary stars with non-coeval components

DOI: DOI

Received ...; revised ...; accepted ..

Abstract: We have estimated masses of components of visual binaries from their spectral classification. We have selected pairs, where the less massive component looks more evolved. Spectral observations of some of such pairs were made, and at least one pair, HD 156331, was confirmed to have components of different age. Since mass exchange is excluded in wide binaries, it means that HD 156331 can be formed by the capture.

Keywords: Binary Stars, Stellar Mass

1 Introduction

The formation of binary stars basically follows two scenarios: fission of rotating molecular gas clouds during gravitational collapse, and inelastic collisions of stars during the formation of young star clusters (Tutukov & Cherepashchuk, 2020). A capture of a component from the field stars is not ruled out in principle either, although it should be relatively rare. Capture occurs when two stars pass close to each other in the presence of a scattering medium that can take in excess kinetic energy, to leave the two stars bound. This medium could be a third star, a circumstellar disk, or the stars themselves, if the collision is close enough to cause the tides to rise and fall. Capture in the presence of a third body and “tidal capture” requires a high stellar density, which is atypical for field stars.

Capture in the presence of a stellar disk may play some role in the formation of wide systems, because the capture cross section has to be on the order of the size of the disk and thus lead to the formation of systems with large semi-axes about 100 AU. Clarke & Pringle (1991) considered the possibility of a large, massive protostellar accretion disc playing a role in the formation of binary stars by enabling the capture of a passing star within a dense star-forming region. It was found that capture rates are too low to play a major role in all known star-

forming environments, particularly when the probability of prior disc dispersal by the more frequent high-velocity interactions is taken into account.

An indicator of the capture could be the difference in the ages of the components. It is evident, in particular, that in evolutionary wide systems (i.e., systems with no matter transfer between components today or in the past) with components of the same age, a less massive component cannot appear to be more evolved.

Our previous attempt to find pairs with non-coeval components was based on estimating the durations of preMS and MS stages for stars of different masses. In particular, we looked for wide pairs where a very low-mass secondary component (with mass m_2 and duration of preMS stage $\tau_{\text{preMS}}(m_2)$) is *already* an MS star, and massive primary (with mass m_1 and duration of preMS + MS stages $\tau_{\text{MS}}(m_1)$) is *still* an MS star. We have found three candidates with $\tau_{\text{preMS}}(m_2) > \tau_{\text{MS}}(m_1)$, the results can be found in Malkov (2000).

The aim of the present study is to use another approach to find non-coeval pairs among visual binaries. For indication of non-coevality we compared spectral classes and masses of the components, estimated from the spectral classification.

The structure of this paper is as follows: in Section 2 we describe our sample selection, in Section 3 we describe our observations for the first three objects and spectral data reductions. Data analysis is described in Section 4, and the results are discussed in Section 5. Section 6 summarizes this paper.

Corresponding Author: Oleg Malkov: Institute of Astronomy, Moscow, Russia; Email: malkov@inasan.ru

Alexei Kniazev: South African Astronomical Observatory, Cape Town, South Africa; Sternberg Astronomical Institute, Moscow, Russia

Table 1. Systems under study. Pairs

Name	V, mag	ϖ , mas	σ_{ϖ}
HD 101379	5.095	8.397	0.507
HD 156331	6.267	16.703	0.048
HD 160928	5.871	13.053	0.599

Parallax ϖ and visual brightness V are taken from Gaia EDR3 and SIMBAD, respectively.

2 Sample selection

The general method of this work is an applying the simple idea to find non-coeval pairs among visual binaries. For indication of non-coevality we compared spectral classes and masses of the components, estimated from the spectral classification. Applying this idea to the Sixth Catalog of Orbits of Visual Binary Stars, ORB6 (Hartkopf et al., 2001), we found thirteen systems where less massive component looks more evolved, and, consequently, the components are probably non-coeval (Malkov, 2020).

We have made a search for additional data on these thirteen systems in ORB6 (Hartkopf et al., 2001), Catalogue of Stellar Spectral Classifications (Skiff, 2014), Multiple star catalogue, MSC (Tokovinin, 2018), as well as in the SIMBAD database. The parameters of three systems presented in this paper are shown in Table 1.

3 Observations and Data Reduction

Three of these thirteen systems have been observed with the Southern African Large Telescope (SALT; Buckley et al., 2006; O’Donoghue et al., 2006) using the High Resolution Spectrograph (HRS; Barnes et al., 2008; Bramall et al., 2010, 2012; Crause et al., 2014). The HRS is a thermostabilized double-beam echelle spectrograph, the entire optical part which is housed in a vacuum to reduce the influence of temperature variations and mechanical interference. The blue arm of the spectrograph covers the spectral range 3735–5580 Å, and the red arm covers the spectral range of 5415–8870 Å, respectively. The spectrograph is equipped with two fibers (object and sky fibers) and can be used in the low (LR, $R \approx 14,000$ –15,000) medium (MR, $R \approx 40,000$ –43,000) and high (HR, $R \approx 67,000$ –74,000) resolution modes. For our observation HRS was used in MR, where for both the object and sky

Table 2. Observational log

Name	Date	Exposure (s)	Seeing (arcsec)	SNR
HD 101379	2021 July 14	3×25	1.5	150–400
HD 156331	2021 May 10	1×40	1.1	150–280
HD 160928	2021 May 10	1×40	1.2	200–300

fibers have 2.23 arcsec in diameter. The both blue and red arms CCD were read out by a single amplifier with a 1×1 binning. All additional details of observations are summarized in the Table 2. Generally, each star was observed once, but in case HD 101379 three spectra were obtained, where for both HD 156331 and HD 160928 only one spectrum was obtained. Exposures were selected in the way to accumulate Signal-to-Noise Ratio (SNR) more than 150 in the spectral region 4300–8800 Å. Unfortunately, sensitivity of HRS drops down fast bluer of 4300 Å and the final SNR in this spectral region is very hard to predict.

Three spectral flats and one spectrum of ThAr lamp were obtained in this mode during a weekly set of HRS calibrations that enough to get average external accuracy of 300 m s^{-1} . Method of analysis, described in Section 4 needs to use spectra corrected for sensitivity curve. For this reason spectra of spectrophotometric standard from the list of Kniazev (2017)¹ were observed and used during HRS data reduction.

Primary reduction of the HRS data, including over-scan correction, bias subtractions and gain correction, was done with the SALT science pipeline (Crawford et al., 2010). Spectroscopic reduction of the HRS data was carried out using standard HRS pipeline and our own additions to it described in details in (Kniazev et al., 2019).

4 Spectral Data Analysis

Analysis of totally reduced HRS spectra was done with a dedicated software package fbs (Fitting Binary Stars; Kniazev et al., 2020) developed by our team for the stellar spectra analysis and used by us in the different studies (Berdnikov et al., 2019; Gvaramadze et al., 2019; Kniazev, 2020; Gvaramadze et al., 2021). This software is fitted observed spectra with use of the library of high-resolution theoretical stellar spectra and is designed to derive radial velocities and stellar parameters

¹ <https://astronomers.salt.ac.za/software/hrs-pipeline/>

Table 3. Stellar parameters found with `fb`s software

System	T_{eff} (K)	$\log g$ (cm s^{-1})	$V \sin i$ (km s^{-1})	V_{hel} (km s^{-1})	Weight in V band	M_V (mag)	[Fe/H] (dex)	$E(B - V)$ (mag)	St. lib.
HD 101379 A	5160 ± 100	4.1 ± 0.19	3.0 ± 0.2	-6.1 ± 0.3	0.73 ± 0.01	-0.69 ± 0.13	0.42 ± 0.18	0.24 ± 0.01	Coelho
HD 101379 A	5000 ± 25	3.8 ± 0.01	10.4 ± 0.2	-5.9 ± 0.2	0.72 ± 0.01	-0.70 ± 0.13	0.19 ± 0.01	0.25 ± 0.01	Phoenix
HD 101379 B	10460 ± 55	4.6 ± 0.08	104.5 ± 2.3	30.5 ± 0.4	0.27 ± 0.01	0.39 ± 0.13	0.42 ± 0.18	0.24 ± 0.01	Coelho
HD 101379 B	10230 ± 180	3.9 ± 0.03	90.3 ± 0.9	30.3 ± 0.3	0.28 ± 0.01	0.32 ± 0.13	0.19 ± 0.01	0.25 ± 0.01	Phoenix
HD 156331 A	6000 ± 10	4.0 ± 0.01	35.1 ± 0.2	9.8 ± 0.2	0.72 ± 0.01	2.74 ± 0.01	-0.28 ± 0.01	0.00 ± 0.01	Coelho
HD 156331 A	5990 ± 10	3.8 ± 0.06	36.8 ± 0.2	9.9 ± 0.1	0.68 ± 0.01	2.80 ± 0.01	-0.20 ± 0.02	0.00 ± 0.01	Phoenix
HD 156331 B	8190 ± 20	3.8 ± 0.03	60.8 ± 0.3	33.7 ± 0.2	0.28 ± 0.01	3.76 ± 0.01	-0.28 ± 0.01	0.00 ± 0.01	Coelho
HD 156331 B	8010 ± 20	4.0 ± 0.04	60.0 ± 0.3	31.1 ± 0.3	0.32 ± 0.01	3.62 ± 0.01	-0.20 ± 0.02	0.00 ± 0.01	Phoenix
HD 160928 A	8270 ± 10	3.7 ± 0.02	238.4 ± 0.7	-7.3 ± 0.3	0.79 ± 0.01	1.71 ± 0.10	-0.34 ± 0.01	0.00 ± 0.01	Coelho
HD 160928 A	8450 ± 20	3.9 ± 0.01	225.0 ± 0.8	-8.5 ± 1.3	0.73 ± 0.01	1.79 ± 0.10	-0.15 ± 0.03	0.00 ± 0.02	Phoenix
HD 160928 B	6400 ± 20	4.5 ± 0.06	173.5 ± 0.5	-15.4 ± 0.6	0.21 ± 0.01	3.14 ± 0.10	-0.34 ± 0.01	0.00 ± 0.01	Coelho
HD 160928 B	6880 ± 60	4.8 ± 0.01	190.3 ± 1.5	-16.5 ± 1.6	0.27 ± 0.01	2.87 ± 0.10	-0.15 ± 0.03	0.00 ± 0.02	Phoenix
Errors	300.	0.35	10.	1.3	0.02		0.06	0.01	

(T_{eff} , $\log g$, $\sin i$ and [Fe/H]) for each component of a binary system. In clear cases of binary stars, the package uses two model spectra with individual velocities and stellar parameters. As an output software produces velocities and stellar parameters for both components. The current version of this software is using different stellar models (Coelho, 2014; Husser et al., 2013; Hubeny & Lanz, 1995).

It was noted in Kniazev (2020) that output errors of the `fb`s are errors of fitting, which are often underestimate the real errors. Unfortunately, since each reduced échelle spectrum is about hundred thousands points length, the way to find a global minimum of the function shown in Kniazev et al. (2020) is very time-consuming process. For that reason, Monte-Carlo simulations or use of Markov chain Monte Carlo methods are not a real way to estimate errors. It is easier to estimate accuracy of the method comparing results of `fb`s with previously published data (for example, see Kniazev et al., 2020) or to use each obtained spectrum of the same object as an independent one, model each with `fb`s and study the output result as the statistical sample (Kniazev, 2020).

The results of our `fb`s modeling for obtained spectra are presented in Table 3 and shown in Fig. 1. Since three spectra were obtained for HD 101379, each spectrum was analyzed with `fb`s independently and presented parameters and their errors are average values for this star. We also repeated the same analysis with both Coelho (2014) (COELHO in Table 3) and (Husser et al., 2013) stellar models (PHOENIX in Table 3), convolving them to match the HRS MR instrumental resolution. These results are also presented in Table 3. Finally, after comparison these re-

sults we use errors for each parameter in this work as they shown in the last row of Table 3.

5 Parameters of the studied systems

The parameters of three systems observed with SALT are shown in Fig. 2 and presented in Tables 1 and 3. Absolute magnitudes of the components M_V are calculated from parallax and visual brightness (see Table 1) and from weight in V band and interstellar reddening $E(B - V)$ values (see Table 3).

We can see from Fig. 2 that more massive (and more luminous) components of HD 101379 and HD 160928 look more evolved than the less massive ones. It should be added that according to MSC (Tokovinin, 2018), HD 101379 (= WDS 11395-6524 = HIP 56862) is in fact a quadruple system, where HD 101379 A is a spectroscopic binary SB1, and HD 101379 B is an eclipsing binary.

Contrary, the secondary (less massive) component of HD 156331 is more evolved than the primary (see Fig. 2), and, consequently, it is a good candidate to the wide binary with non-coeval components. It is an indication of the non-coevality of the components and, consequently, we can assume that this system could be formed by a capture.

In addition, another assessment can be made. HD 156331 was included in our list of pairs with probably non-coeval components (Malkov, 2020) because the spectral classification of the components, F8III+B9V, given in WDS (Mason et al., 2001), corresponds to masses of 1.76 and 2.58 (hereafter in solar mass), respectively, and hence the less massive component looks more evolved. The val-

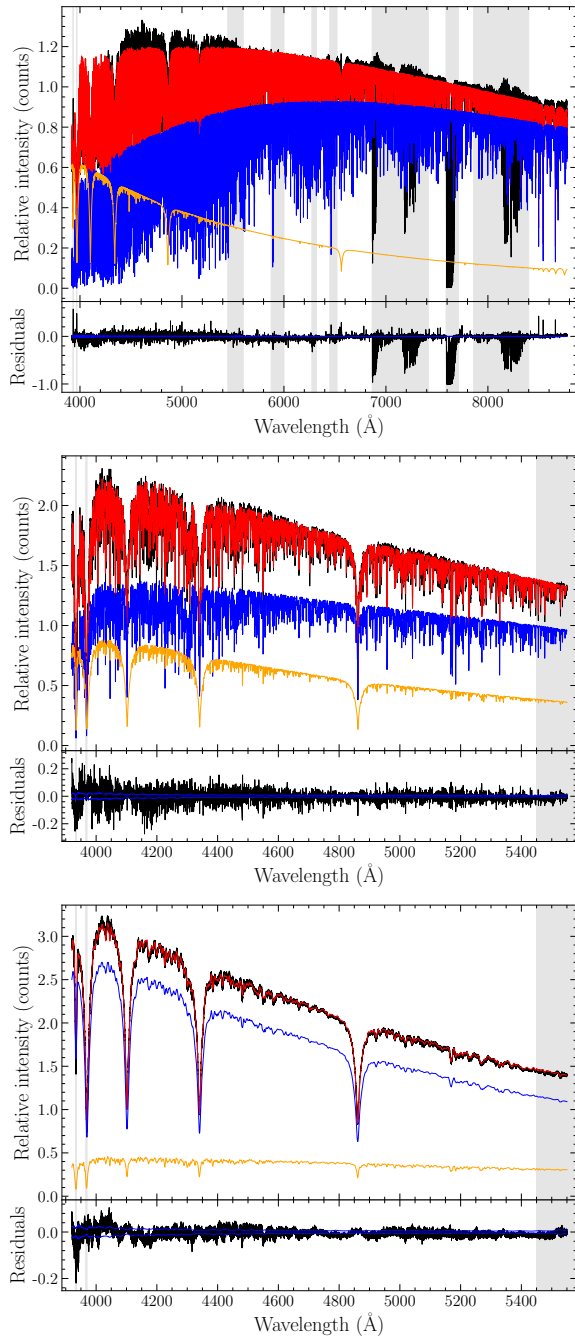


Fig. 1. The results of the fbs fit all stars from this work: HD 101379 (top), HD 156331 (middle) and HD 160928 (bottom). Each panel consists of two sub-panels: **the top one** shows the result of the fit in the spectral region 3900-8870 Å. The observed spectrum is shown in black. Both found components are shown in blue and orange respectively, where their sum is shown in red. **the bottom one** shows the difference between the observed spectrum and its model in black, altogether with errors that were propagated from the HRS data reduction (continuous dark blue line). Grey vertical areas mark the spectral ranges that were excluded from the fit for different reasons, mainly due to bands of lines from the Earth atmosphere. Only blue spectra are shown for HD 156331 and HD 160928 just for more details.

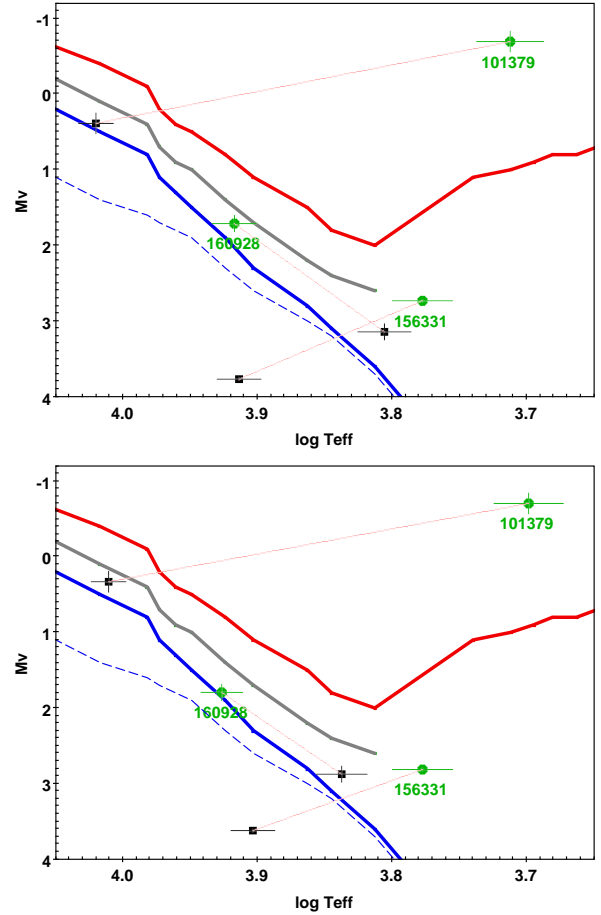


Fig. 2. HD 101379, HD 156331 and HD 160928 systems on the HRD. Solid curves represent main sequence, subgiant and giant sequences (blue, grey and red, respectively), and dashed blue curve represents ZAMS (Straižys, 1992). Green circles and black squares represent primary (more luminous) and secondary components of the binaries, respectively, with uncertainty bars. Top and bottom panels: Coelho and Phoenix stellar models, respectively.

ues of T_{eff} , $\log g$ obtained in this work for this system (see Table 3, Phoenix library) rather indicate the spectral types F5III+A7IV, which corresponds to masses of 1.51 and 1.82. The difference in masses has decreased, but the situation has not changed qualitatively. Here we use the scales $\text{SpT} - T_{\text{eff}} - \log g - \text{mass}$ from (Straizys, 1992), the typical mass error value when estimating it from the spectral type is 0.1.

However, the assumption that HD 156331 B has LC=IV or V contradicts with its position on the HRD (see Fig. 2). The star is located well below ZAMS. According to WDS (Mason et al., 2001), the components of HD 156331 have the same brightness in the V-band (which is contrary to our Weight values in Table 3), but even under this assumption absolute magnitude of HD 156331 B “rises” only to a value of $M_V = 3.13$ mag and the star remains under ZAMS.

In his detailed study of several fast visual binaries, based on speckle interferometry, Tokovinin (2017), in particular, found orbital elements and calculated dynamical parallax for HD 156331 ($\varpi_{\text{dyn}} = 14.2$ mas), which turned out to be different from the Hipparcos value ($\varpi_{\text{HIP}} = 16.9$ mas). The recent Gaia observations rather confirm the latter value ($\varpi_{\text{Gaia}} = 16.7$ mas, see Table 1 and note that the parallax is given with a fairly high accuracy, 3%). But even relying on dynamical parallax will only make the components brighter by about 0.3 mag, and HD 156331 B will still remain under ZAMS in Fig. 2.

Our values of HD 156331 components’ radial velocities (see Table 3) are quite consistent with RV difference of $\sim 30 \text{ km s}^{-1}$ near the periastron, predicted by Tokovinin (2017). Contrary, components’ magnitude difference found by Tokovinin (2017) corresponds to WDS values and not to values, found in this paper and given in Table 3.

Finally, it should be pointed out that the formal errors derived from the separation of the spectra of the parameters of the components significantly underestimate the real ones. Moreover, the output parameters can be correlated (for example, $\log g$ and $V \sin i$), so the analysis of the position of the components on the HRD must take into account the errors of the total brightness, and of the magnitude difference, as well as errors and a possible correlation of the obtained temperatures.

So the HD 156331 system requires further observation and analysis.

6 Conclusion

We have studied several stars from our preliminary list of candidates to wide pairs with non-coeval components, and we have found that the less massive component of HD 156331 is probably more evolved than the more massive. We can assume that this system could be formed by a capture. To prove the non-coequality one needs a detailed investigation of this and other candidates.

7 Acknowledgments

We are grateful to our anonymous reviewer whose constructive comments greatly helped us to improve the paper. All spectral observations reported in this paper were obtained with the Southern African Large Telescope (SALT) under program 2020-1-MLT-002 (PI: Alexei Kniazev). The work was partly supported by the Russian Foundation for Basic Researches (project 19-07-01198). A. K. acknowledges support from the National Research Foundation (NRF) of South Africa. This research has made use of NASA’s Astrophysics Data System, of the SIMBAD database, operated at CDS (Strasbourg, France), of TOPCAT, an interactive graphical viewer and editor for tabular data (Taylor, 2005). The acknowledgements were compiled using the Astronomy Acknowledgement Generator.

References

- Barnes, S. I., Cottrell, P. L., Albrow, M. D., et al. 2008, Society of Photo-Optical Instrumentation Engineers (SPIE) Conference Series, Vol. 7014, The optical design of the Southern African Large Telescope high resolution spectrograph: SALT HRS, Society of Photo-Optical Instrumentation Engineers (SPIE) Conference Series, Vol. 7014, Ground-based and Airborne Instrumentation for Astronomy II. Edited by McLean, Ian S.; Casali, Mark M. Proceedings of the SPIE, Volume 7014, article id. 70140K, 12 pp. (2008)., 70140K
- Berdnikov, L. N., Kniazev, A. Y., Dambis, A. K., et al. 2019, *Astrophysical Bulletin*, 74, 183
- Bramall, D. G., Sharples, R., Tyas, L., et al. 2010, Society of Photo-Optical Instrumentation Engineers (SPIE) Conference Series, Vol. 7735, The SALT HRS spectrograph: final design, instrument capabilities, and operational modes, Society of Photo-Optical Instrumentation Engineers (SPIE) Conference Series, Vol. 7735, Proceedings of the SPIE, Volume 7735, id. 77354F (2010)., 77354F
- Bramall, D. G., Schmoll, J., Tyas, L. M. G., et al. 2012, Society of Photo-Optical Instrumentation Engineers (SPIE) Confer-

- ence Series, Vol. 8446, The SALT HRS spectrograph: instrument integration and laboratory test results, Society of Photo-Optical Instrumentation Engineers (SPIE) Conference Series, Vol. 8446, Ground-based and Airborne Instrumentation for Astronomy IV. Proceedings of the SPIE, Volume 8446, article id. 84460A, 9 pp. (2012)., 84460A
- Buckley, D. A. H., Swart, G. P., & Meiring, J. G. 2006, Society of Photo-Optical Instrumentation Engineers (SPIE) Conference Series, Vol. 6267, Completion and commissioning of the Southern African Large Telescope, Society of Photo-Optical Instrumentation Engineers (SPIE) Conference Series, Vol. 6267, Ground-based and Airborne Telescopes. Edited by Stepp, Larry M.. Proceedings of the SPIE, Volume 6267, id. 62670Z (2006)., 62670Z
- Clarke, C. J., & Pringle, J. E. 1991, *MNRAS*, 249, 584
- Coelho, P. R. T. 2014, *MNRAS*, 440, 1027
- Crause, L. A., Sharples, R. M., Bramall, D. G., et al. 2014, Society of Photo-Optical Instrumentation Engineers (SPIE) Conference Series, Vol. 9147, Performance of the Southern African Large Telescope (SALT) High Resolution Spectrograph (HRS), Society of Photo-Optical Instrumentation Engineers (SPIE) Conference Series, Vol. 9147, Proceedings of the SPIE, Volume 9147, id. 91476T 14 pp. (2014)., 91476T
- Crawford, S. M., Still, M., Schellart, P., et al. 2010, Society of Photo-Optical Instrumentation Engineers (SPIE) Conference Series, Vol. 7737, PySALT: the SALT science pipeline, Society of Photo-Optical Instrumentation Engineers (SPIE) Conference Series, Vol. 7737, Proceedings of the SPIE, Volume 7737, id. 773725 (2010)., 773725
- Gvaramadze, V. V., Kniazev, A. Y., Gallagher, J. S., et al. 2021, *MNRAS*, 503, 3856
- Gvaramadze, V. V., Maryeva, O. V., Kniazev, A. Y., et al. 2019, *MNRAS*, 482, 4408
- Hartkopf, W. I., Mason, B. D., & Worley, C. E. 2001, *AJ*, 122, 3472
- Hubeny, I., & Lanz, T. 1995, *ApJ*, 439, 875
- Husser, T. O., Wende-von Berg, S., Dreizler, S., et al. 2013, *A&A*, 553, A6
- Kniazev, A. 2020, *Astrophysics and Space Science*, 365, 169
- Kniazev, A. Y. 2017, *SALT Report*, 1
- Kniazev, A. Y., Malkov, O. Y., Katkov, I. Y., & Berdnikov, L. N. 2020, *Research in Astronomy and Astrophysics*, 20, 119
- Kniazev, A. Y., Usenko, I. A., Kovtyukh, V. V., & Berdnikov, L. N. 2019, *Astrophysical Bulletin*, 74, 208
- Malkov, O. 2000, in *IAU Symposium*, Vol. 200, *IAU Symposium*, 170
- Malkov, O. Y. 2020, *INASAN Science Reports*, 5, 341
- Mason, B. D., Wycoff, G. L., Hartkopf, W. I., Douglass, G. G., & Worley, C. E. 2001, *AJ*, 122, 3466
- O'Donoghue, D., Buckley, D. A. H., Balona, L. A., et al. 2006, *MNRAS*, 372, 151
- Skiff, B. A. 2014, *VizieR Online Data Catalog*, B/mk
- Straižys, V. 1992, *Multicolor stellar photometry* (Tucson : Pachart Pub. House, 1992.)
- Taylor, M. B. 2005, in *Astronomical Society of the Pacific Conference Series*, Vol. 347, *Astronomical Data Analysis Software and Systems XIV*, ed. P. Shopbell, M. Britton, & R. Ebert, 29
- Tokovinin, A. 2017, *AJ*, 154, 110
- Tokovinin, A. 2018, *ApJS*, 235, 6
- Tutukov, A. V., & Cherepashchuk, A. M. 2020, *Physics Uspekhi*, 63, 209